*Pakistan J. Zool., vol. 53(6), pp 2021-2031, 2021* **DOI**: https://dx.doi.org/10.17582/journal.pjz/20190514070541

# Cloning, Expression, Purification, and Characterization of Soluble Bioactive Recombinant Human Anterior Gradient Homolog 2 - DsRed Monomer Protein in *Escherichia coli*

**Bingjie Zhou[1], Hitesh Bhagavanbhai Mangukiya[1], Siva Bharath Merugu[1], Fakhar-un-Nisa Yunus[1], Yuchen Fan[1], Zhenghua Wu[1,*] and Dawei Li[1,2,*]**

[1]*School of Pharmacy, Shanghai Jiao Tong University, Shanghai, China.*
[2]*Engineering Research Center of Cell and Therapeutic Antibody of Ministry of Education, School of Pharmacy, Shanghai Jiao Tong University, Shanghai, China.*

**Bingjie Zhou and Hitesh Bhagavanbhai Mangukiya contributed equally to this article.**

**Article Information**
**Received 14 April 2019**
**Revised 16 May 2019**
**Accepted 31 May 2019**
**Available online 03 September 2021**

**Authors' Contribution**
**All the authors contributed to the designing of the research. BZ, HBM and SBM conducted the research and analyzed data. BZ and HBM wrote the paper with the inputs from SBM and YF. ZW and DL obtained funding for this work.**

**Key words**
**Anterior gradient homolog 2, Red fluorescent protein, Recombinant expression, *Escherichia coli***

## ABSTRACT

Anterior gradient 2 (AGR2), initially discovered as an estrogen-responsive gene in breast cancer cell lines, is a developmentally regulated gene belonging to the protein disulfide isomerase (PDI) gene family. AGR2 exists in both intracellular and secreted form, it is overexpressed in many types of cancer cells and also detected in extracellular space of solid tumor interstitial fluids. The intracellular AGR2 is critical in protein folding while secreted AGR2 function as a paracrine signal promoting tumor microenvironment formation. Beside cancer progression and drug resistance, the abnormal expression of AGR2 is also involved in diseases like asthma and inflammatory bowel disease. Studies on the role of AGR2 in tumor micro-environment can help potential therapeutic development. Here, we report the generation of a fluorescent functional AGR2 fusion protein as a powerful visual tracking tool to trace the external function of AGR2. This bioactive and auto-fluorescent his-tag recombinant AGR2-DsRed (hAD) protein was constructed by linking human AGR2 C-terminus with the red fluorescent protein derived from *Discosoma sp.* (DsRed) through a flexible linker. It was expressed successfully in *Escherichia coli* (*E. coli*) with optimized strain and cultivation parameters. This protein was expressed and purified by Nickel-nitroacetic acid (Ni-NTA) affinity chromatography. The bioactivity of AGR2 was tested by cell proliferation and wound healing assays, while the auto-fluorescent property of DsRed was confirmed by fluorescence microscopy and immunofluorescence. The potential application of his-AGR2-DsRed was demonstrated by its internalization in fibroblasts. Therefore, the purified recombinant fluorescent protein would be a very useful tool for further investigation of AGR2's extracellular function and molecular mechanism.

## INTRODUCTION

The human anterior gradient-2 (AGR2) is an orthologue of the Xenopus Anterior Gradient-2 (XAG-2) protein which is predominantly found in tissues with endocrine cells or mucus-secreting cells, such as colon, rectum, stomach, breast, and prostate (Fritzsche *et al*., 2006; Brychtova *et al*., 2011). AGR2 belongs to the protein disulfide isomerase family (PDI), which is physiologically localized in endoplasmic reticulum (ER). AGR2 has been discovered to regulate the body appendages regeneration in amphibian and regulation of limb and tail regeneration in Xenopus laevis tadpoles and limb regeneration in salamander (Kumar *et al*., 2007; Ivanova *et al*., 2013). In context of cancer, AGR2 was originally studied in human breast cancer (Kuang *et al*., 1998). AGR2 contains both the ER retention sequence KTEL, and the secretory signal-peptide which has been investigated to be over expressed in various human cancer types (Brychtova *et al*., 2011; Chevet *et al*., 2013). Cancer-related functions of intracellular AGR2 have been investigated intensively (Higa *et al*., 2011; Chevet *et al*., 2013; Brychtova *et al*., 2015).

It has been reported that AGR2 secreted by Gastric signet-ring carcinoma cells mediates the paracrine effects on stromal fibroblasts that promote invasion (Tsuji *et al*., 2015). This ER-resident protein secreted in cancer microenvironment triggers novel signaling pathways that exhibit pro-oncogenic gain-of-functions in cancer (Ramachandran *et al*., 2008; Dumartin *et al*., 2011).

* Corresponding author: daweili@sjtu.edu.cn; wuzhenghua@sjtu.edu.cn
0030-9923/2021/0006-2021 $ 9.00/0

Previously, it has been investigated that tumor-secreted AGR2 binds to VEGF and FGF2 and enhances their functional activities by promoting homodimerization (Guo *et al*., 2017). Another study showed that secreted AGR2 promotes colorectal cells invasion via Wnt11-mediated non-canonical Wnt signaling (Tian *et al*., 2018). Whereas, role of extracellular AGR2 in tumorigenesis and molecular mechanism remains poorly understood. The lack of well-designed bioactive recombinant AGR2 makes it difficult to discover the paracrine signaling mechanism for *in vitro* and *in vivo* studies. To investigate the paracrine signaling of AGR2 and study the molecular mechanism in tumor microenvironment, it is necessary to design and construct a bioactive recombinant fluorescence AGR2 protein.

Fluorescent proteins are easily imaged reporters crucial in biology and biotechnology (Tsien, 1998; Zhang *et al*., 2002), and recent studies has shown the tremendous advantages of the newly cloned red fluorescence protein DsRed from the *Discosoma* genus: bright red fluorescence and high resistance against photo bleaching (Baird *et al*., 2000; Lounis *et al*., 2002). However, when a protein is fused to a fluorescent protein, interactions between fluorescent proteins may undesirably disturb targeting or function (Lauf *et al*., 2001). Since all wild-type yellow-to-red fluorescent proteins reported so far are obligately tetrameric and often toxic or disruptive (Matz *et al*., 1999; Baird *et al*., 2000), the red fluorescent monomer, which derived from DsRed by directed evolution first to increase the speed of maturation (Bevis *et al*., 2002), was chosen in this study.

AGR2 is located on chromosome 7p21, a region known to have frequent genetic alterations (Petek *et al*., 2003). In recent years, the researchers focus on developing bioactive recombinant protein secreted by cancer cells to investigate signaling mechanism of these onco-proteins for betterment of therapeutics. For these purpose, we aimed to design a bioactive recombinant AGR2 fluorescent protein.

We cloned, expressed, purified, and characterized his-AGR2-DsRed. We successfully optimized expression of novel recombinant hAD fluorescent protein using *Escherichia coli* plasmid expression system. We characterized hAD to check its bioactivity showing migration of NIH3T3 cells increased by hAD and its internalization by A549 as well as NIH3T3 cells. Thus, this recombinant hAD fluorescent protein can potentially be used to study paracrine signaling mechanism in context of cancer development which will lead to design most effective cancer treatment.

## MATERIALS AND METHODS

*Molecular cloning of human AGR2*

Total RNA was isolated from human breast adenocarcinoma cell line MCF7, then reverse transcription

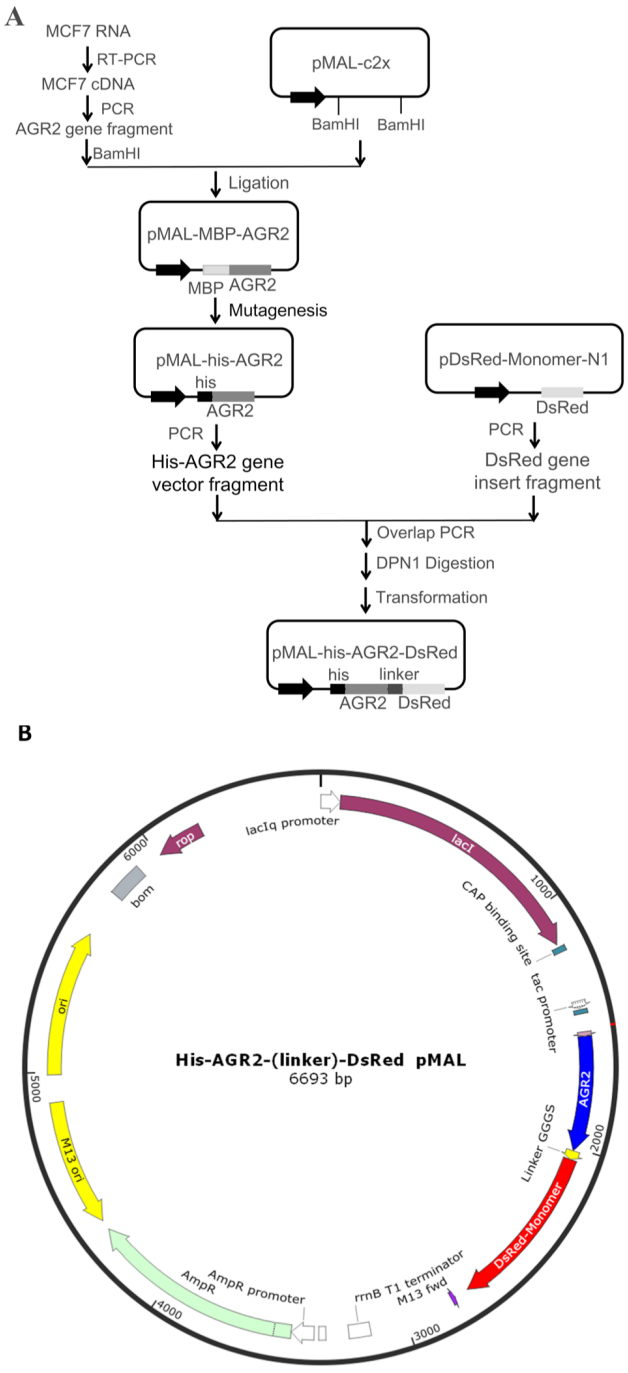


Fig. 1. Construction and cloning of his-AGR2-DsRed plasmid. (A) Flowchart for the construction of his-AGR2-DsRed plasmid. (B) A schematic representation of his-AGR2-DsRed plasmid map. Essential elements include a poly-histidine tag, human AGR2 gene without signal peptide, a $(GGGS)_3$ flexible linker, DsRed monomer gene as well as genes encoding the LacI repressor (*lac*R), ampicillin resistance (AmpR) and origins of replication.

was performed using a ReverTra Ace qPCR RT Kit (TOYOBO). Native human AGR2 open reading frame was PCR amplified from MCF7 cDNA using hAGR2-AMP-F (5'-GGATCCATGGAGAAAATTCCAGTGTC-3') and hAGR2-AMP-R (5'-TTACAATTCAGTCTTCAGCA-3'). Here, the signal peptide (amino acids 1–20) was truncated to mimic the mature secreted protein. A modified pMAL-his-△MBP plasmid, where the MBP (maltose binding protein) tag in pMAL-c2x (NEB, USA) was delated and replaced by a 6×his (histidine) tag, was generated by our lab. The resulting PCR product was cloned into the modified pMAL-his-△MBP plasmid, by restriction enzyme cutting and ligation, resulting in an N-terminal 6-histidine-human AGR2 protein expression construct named as pMAL-his-AGR2.

*Cloning of DsRed into pMAL-his-AGR2 plasmid*

DsRed gene was preceded by human AGR2 gene fused at the N-terminus to a 6×his tag (Fig.1). To make sure the recombinant hAD protein can be expressed efficiently, a flexible linker $(GGGS)_3$ was designed between human AGR2 and DsRed monomer region.

The insert DsRed gene fragment from pDsRed-monomer-N1 (Clontech, Takara Bio, USA) and vector fragment containing his-AGR2 from pMAL-his-AGR2 plasmid described above was PCR amplified with KOD -Plus- 1207 (TOYOBO, Japan), using "chimeric" primers, characterized by sequences that overlap with each other, and regions complementary to the template (Table I).

The PCR products were then purified through DNA gel extraction kit (Solarbio, China) and checked by agarose gel electrophoresis. The vector and insert fragments were mixed with a molar ratio of 1:5 respectively, and linked by overlap PCR. After digesting the residual template for 1h at 37°C with Dpn I (TOYOBO, Japan), the DNA was then transformed into DH5α (#CB101, TIANGEN, China) and BL21 (DE3) (#CB105, TIANGEN, China) *E. coli* competent cells. Successful cloning was confirmed by sequencing (Personalbio, China).

*Expression of hAD in* E. coli

A single colony of transformed cells was inoculated into 2mL of Luria-Bertani (LB) broth media and grown at 37℃ and 150 rpm overnight. Then the overnight culture was inoculated with a ratio of 1:100, cultured at 37℃ with 150 rpm agitation until reaching $OD_{600}$ = 0.6~0.8, induced with 1 mM isopropyl β-D-thiogalactoside (IPTG) (SolarBio, China) and grown for a further 4h. Different strains, IPTG concentrations and inducing time were tested to get the optimized condition. 300μl aliquots were centrifuged at ~10000×*g* for 1 minute (min), the bacteria pellet was resuspended in 100μl phosphate buffered saline (PBS) as induced samples. 1ml aliquots were centrifuged at ~10000×*g* for 1 min, the bacteria pellet was resuspended in 300μl BugBuster® Protein Extraction Reagent (Novagen, Germany), shook for 15 mins at room temperature, centrifuged at ~10000×*g* for 5 min. 100μL supernatant was collected as supernatant samples, producing the soluble fraction. After removing all the supernatant, the pellet remained was resuspended in 300μL PBS and 100μL of the solution was collected as pellet samples. Recombinant protein expression in the soluble and insoluble fractions was analyzed by sodium dodecyl sulphate polyacrylamide gel electrophoresis (SDS-PAGE) and Western blot (WB) as described below.

*Large scale expression and Ni-NTA agarose affinity chromatography purification*

Large cultures were produced by inoculating 500 ml LB broth with 5 ml overnight cultures using the expression parameters described above. Cultures were subsequently

**Table I.- Primers used in construction. The primers were synthesized by Personalbio.**

| Template | Primers | Sequence (5' to 3') |
|---|---|---|
| pMAL-his-AGR2 | Forward | **gctcccag**tccggactcTAAAAATCTCTAGAGGATCCTCTTAGAGTCGACCTG |
| | Reverse | *gatcctcctccagaaccaccacc*CAATTCAGTCTTCAGCAACTTGAGAGC |
| pDsRed-Monomer-N1 | Forward | *gtggttctggaggaggatcaggcggcggatcc***ATGGACAACACCGAGGACGTC** |
| | Reverse | ctagaggatcctctagagatttttagagtccgg**ACTGGGAGCCGGAGTGG** |
| Annotation | Lower case: appended overlap sequence | |
| | Capital letters: template annealing sequence | |
| | **Bold**: pDsRed-Monomer-N1 plasmid annealing sequence | |
| | *Italic*: linker sequence | |
| | Underline: stop codon | |

centrifuged at 4°C for 10 min at 10,000×g. The resulting pellet was frozen until use. Prior to purification, every 1g bacteria pellet was thawed, resuspended in 10mL PBS, with 1mL 100mg/mL lysozyme for cell lysis, 100µL 100mM PMSF to inhibit protein degradation and 400µL 25% TritonX-100 to partially dissolve inclusion body. The mixture was left to incubate in ice bath for 30min, sonicated at 400W power, 3 sec on then 6 sec off for in total 10 min and centrifuged at 4°C for 20 min at 10,000×g. The supernatant containing the soluble fraction (crude extract) was decanted, filtered through a 0.2 µm filter and purified as below.

The supernatant containing hAD was loaded onto a Ni-NTA column (SMART Lifesciences, China) pre-incubated with charge buffer and binding buffer. The loaded column was washed with 20 mL of binding buffer and 25 mL of wash buffer containing 60 mM imidazole to remove weakly bound nonspecific proteins. Recombinant hAD was eluted with 6 to 10 mL of elution buffer containing 1M imidazole. Imidazole was then removed by buffer exchanging, and the protein was concentrated by centrifugation in Amicon Ultra 35,000 MWCO concentrators (Millipore, Merck, Germany). Concentration and quality were assessed mainly by SDS-PAGE.

*SDS-PAGE and western blot analysis*

Protein purity was assessed by SDS-PAGE gels and western blots using an anti-AGR2 antibody. Protein samples were separated on standard 12% Tris-glycine SDS-PAGE with β-mercaptoethanol and 5 min heating at 95℃. Samples were run on SDS-PAGE for 35 min at 80V first and separated for 40 min at 120V followed by Coomassie blue staining.

For WB, proteins were separated using SDS–PAGE and transferred onto nitrocellulose membrane and blocked for 1h prior to 2h incubation with primary antibody (1:1000 dilution, monoclonal mouse anti-AGR2, Santa Cruz Biotechnology, USA). Unbound antibody was removed by 3 × 10 min washes with TNE-T before 45min incubation at RT with secondary antibody (1:20000 dilution, goat anti-mouse IgG, LI-COR, USA) and the membrane washed as previously. Antibody detection was performed using Odyssey® CLx Imaging System (LI-COR, USA).

*Fluorescence microscopy*

10µL bacteria culture was dropped on a glass slide, and let stand for 10 min to dry the edge. Then pictures were taken using Epi-Fluorescence microscope (Olympus Inverted Microscopes Models IX71, Japan), Canon digital camera DS126311 and Canon EOS Utility 600D (Canon, Japan).

*Wound healing assay*

NIH3T3 cells (ATCC/CCL-185) were grown till 80~90% confluence reached. After 24h serum starvation, physical gaps were created within a cell monolayer. After given hAD treatment, the process of cell migration into the gap was captured by taking photos at different time points. To ensure that the similar wound areas were compared, the produced wound area was traced and measured by using Image J software (version 1.8.0, http://imagej.nih.gov/ij/; provided in the public domain by the National Institutes of Health, USA) for the multiple positions within each well (Schneider *et al*., 2012). Time-lapse images for each position in the wells were analyzed and the wound areas were measured to determine the percentage of wound closure at several time points throughout the course of the assay. The wound closure by NIH3T3 cells in response to hAD at various concentrations was compared to that of medium containing PBS as a vehicle control.

*Cell proliferation assay*

The bioactivity of recombinant hAD was tested on NIH3T3 fibroblast cells using cell counting kit-8 assay. Around 5000 cells per well were seeded in 96-well plates and subjected to different treatments for 24 hours. 10 µL CCK-8 (Beyotime, China) was added to each well. The plates were then incubated for 4 hours in 37°C. The absorbance value at the wavelength of 6000 nm was measured using a microplate reader (Thermo Fisher Scientific, USA). The cell proliferation percentage was calculated by the ratio of the reported value and the control value.

*The internalization of hAD*

Around $5\times10^5$ NIH3T3 or A549 cells (ATCC/CRL-1658) were seeded in 6-well plates and cultured in DMEM complete media till completely attached. After 24h serum starvation, they were treated with 2 or 5µg/mL hAD for another 24h. Whole cell lysate was prepared using NP-40 lysis buffer added with protease inhibitor (Sigma-Aldrich, Merck, Germany). Proteins were separated using SDS–PAGE and transferred onto nitrocellulose membrane for antibody detection. Mouse monoclonal antibodies against AGR2 and β-actin were purchased from Santa Cruz.

*Immunofluorescence assay*

NIH3T3 cells were grown on coverslips, serum starved for 24h and treated with different concentrations of hAD for 24h. They were then fixed with 4% formaldehyde for 10 min and blocked with goat serum for 30 min. Nuclei were counterstained using DAPI (Invitrogen, USA). The fluorescence was observed and captured with laser confocal microscopy (Leica Camera, Wentzler, Germany).

*Statistical analysis*

All values are expressed as mean ± standard deviation (SD). The GraphPad Prism program (version 7.00, GraphPad Software Inc., USA) was used for all statistical analyses, P value determination and graph drawing. A two-tailed Student's t-test was used to compare measurements of groups of samples if appropriate.

## RESULTS

*Construction of hAD recombinant protein eukaryotic expression plasmid*

The open frame region of human AGR2 consists of 175 amino acids, including a signal peptide (1-20) and a mature peptide (21-175) (Gene accession: NP_006399). Based on the cDNA sequence of human AGR2 mature peptide region and DsRed monomer gene, a set of "chimeric" primers were designed (Table I) to amplify the insert and vector fragments. The amplification of the PCR product, as well as the constructed plasmids were primarily confirmed by an electrophoresis (Fig. 2). The successful cloning was confirmed by sequencing of plasmids extracted from different colonies obtained.

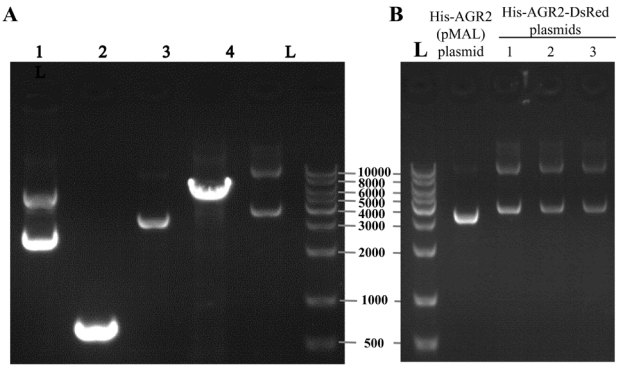


1. pDsRed-Monomer-N1 plasmid
2. DsRed Insert Fragment PCR product
3. pMAL-his-AGR2 plasmid
4. His-AGR2 Vector Fragment PCR product
5. pMAL-his-AGR2-DsRed plasmid

L. DNA Leader

Fig. 2. Agarose gel electrophoresis results of (A) Purified vector and insert fragments and their templates (B) the sequenced right his-AGR2-DsRed plasmids extracted from transformed *E.coli*. Line 1 to 4 were respectively pDsRed-Monomer-N1 plasmid, DsRed insert fragment PCR product, pMAL-his-AGR2 plasmid, his-AGR2 vector fragment PCR product, pMAL-his-AGR2-DsRed plasmid. L represented DNA Leader.

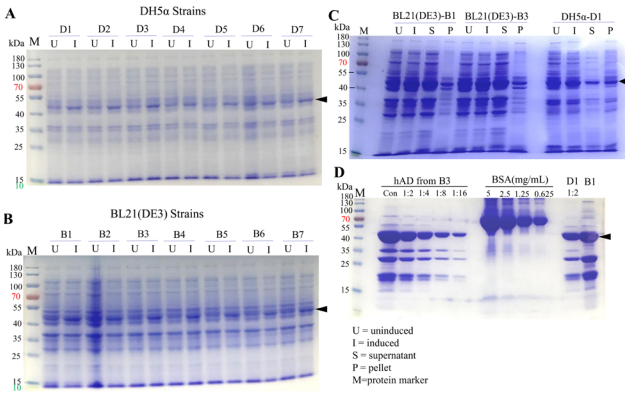


Fig. 3. SDS-PAGE analysis of hAD expression in the BL21 (DE3) and DH5α *E.coli* strains. (A) Expression of hAD tested in DH5α *E.coli,* samples labeled as U were uninduced culture while I represented 1mM IPTG 4-hours induced culture. (B) Expression of hAD tested in BL21 (DE3) *E. coli*. (C) SDS-PAGE result of hAD recombinant protein expression bacteria strains B3 and D1 uninduced-induced samples and expression formats. Recombinant hAD expressed well, with considerable amount of protein being retained in the soluble fractions. (D) Purification results of hAD yielded from 250mL culture under the same conditions and compared with BSA protein standard.

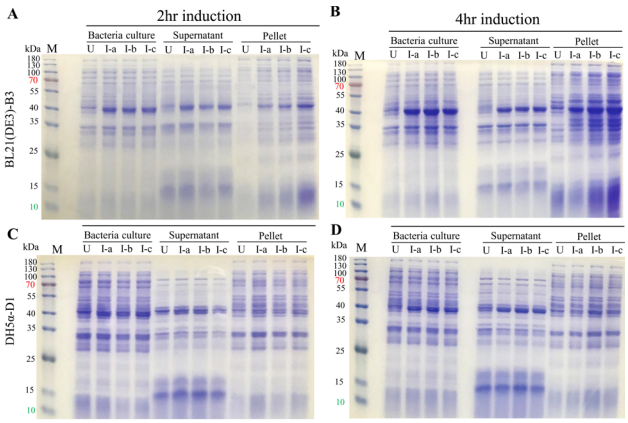


Fig. 4. Optimization of expression condition compared by SDS-PAGE. Samples collected and prepared directly using bacteria culture as well as the expression formats were analyzed by SDS-PAGE. B3 hAD expression strain was cultured and induced under induction of 3 concentrations of IPTG, for 2 hours (A) or 4 hours (B), as well as D1 strain cultured and induced for 2 hours (C) and 4 hours (D). U, uninduced; I, induced; S, supernatant; P, pellet; I-a, 0.1mM IPTG induced; I-b, 0.5mM IPTG induced; I-c, 0.5mM IPTG induced; M, protein marker.

*Comparison of hAD expression in two different* E.coli *strains*

The resulting plasmid from the construction, pMAL-

his-AGR2-DsRed, was transformed into two *E.coli* strains - BL21 (DE3) and DH5α, which originate from different ancestors (B and K12 strain, respectively) and show differences in some metabolic pathways (Pinske *et al.*, 2011) and hAD expression was compared. The aim was to compare expression in the eukaryotic protein expression adapted strain BL21 with the DH5α strain lacking this property. In DH5α strain, less hAD expressed without IPTG induction, and the expression was increased with IPTG induction (Fig. 3A). However, in BL21 (DE3) strain, hAD merely expressed without induction, and after induction the soluble form expressed more than DH5α did (Fig. 3B). From the 14 single colonies, 3 clones were selected for further testing the capacity of hAD expression by SDS-PAGE analysis (Fig. 3C). The expression level in DH5α strain D1 was less than BL21 (DE3) strains B1 and B3, but the supernatant contained less truncation products (also indicated in Figures 4A,B,C,D). D1, B1and B3 strains were cultured in larger scale then followed by Ni-NTA affinity chromatography purification and compared by SDS-PAGE (Fig. 3D). While comparable levels of hAD yielded from 250ml culture under the same conditions were observed between 40 to 55kDa, expression in BL21 (DE3) B3 strain resulted in higher amount of soluble protein, suggesting a higher capability of expression in this host. However, expression in DH5α D1 strain resulted in high purity of hAD protein. For this reason, subsequent analyses were conducted using bacteria or protein produced from D1 strain.

*Optimization of hAD expression conditions in* E.coli

To investigate better conditions for protein expression, samples collected under different IPTG concentrations and induction time points were tested by SDS-PAGE. Our results revealed that a relatively longer induction time gave better protein production when compared to two hours induction results with four hours' (Fig. 4 A vs B, C vs D). When compared the whole expression of hAD in BL21 (DE3) and DH5α strains (Fig. 4 I-a, I-b and I-c columns under bacteria culture, B vs D), it showed that BL21 (DE3) strain was yielding more than DH5α strain, but the latter also gave a higher soluble expression ratio which might be due to the lower inclusion body formation led by slower expression. Regarding the effect of IPTG concentration, no significant difference was observed between 0.5 mM IPTG and 1 mM IPTG group according to SDS-PAGE bands density (Fig. 4 D, I-b vs I-c). But the red fluorescence observed under microscopy indicated that 1mM IPTG induction gave high fluorescence implying better expression (Fig. 5 I-b vs I-c).

*Characterization of hAD recombinant protein*

Fluorescence microscopy analyses were performed directly on hAD expression bacteria D1 strain, taking advantage of the fluorescence of DsRed fused at the C-terminal of the fusion protein (Fig. 6A). Compared to

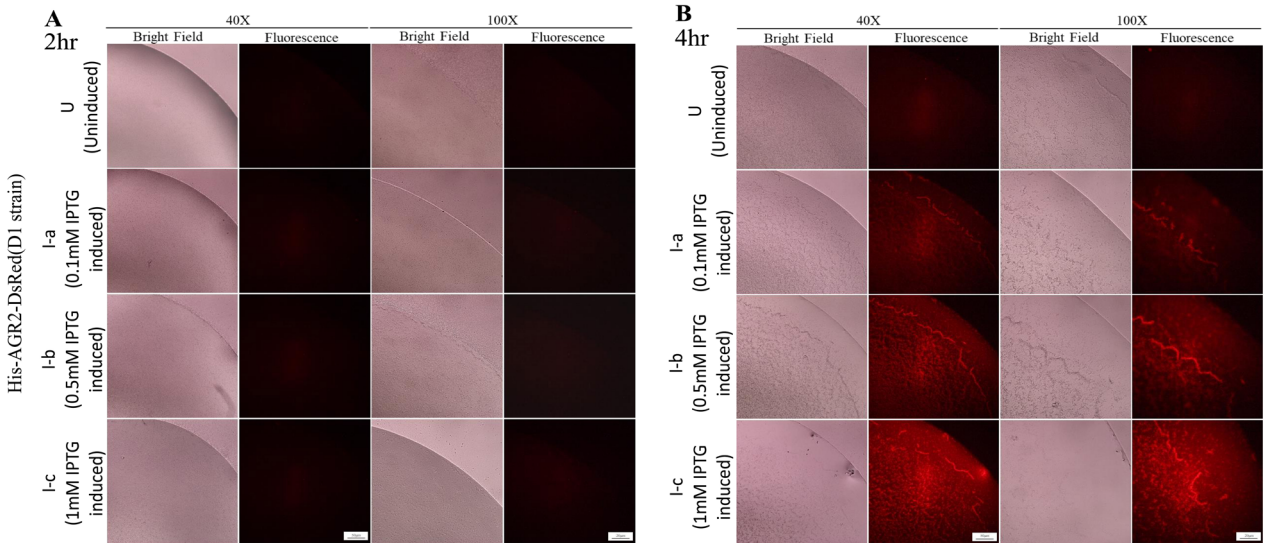


Fig. 5. Optimization of expression condition of hAD in D1 strain compared by fluorescence microscopy. (A&B) D1 hAD expression strain was cultured and induced with 3 different concentrations of IPTG, for 2 hours or 4 hours. The bacterial culture of hAD expression D1 strain were induced for 2 hours or 4 hours aliquoted, observed and recorded under bright field and red fluorescence in 40×magnification. Scale bar, 50μm for 40×magnification and 50μm for 100×magnification. I-a, 0.1mM IPTG induced; I-b, 0.5mM IPTG induced; I-c, 0.5mM IPTG induced.

his-AGR2 expression bacteria culture, the culture drop of D1 strain showed significantly strong red fluorescence under green excitation light, giving obvious visual of bacterial density and distribution. The auto-fluorescence property also allowed the purified protein solution representing crystal red color, while purified his-AGR2 protein solution of the same concentration showed normal colorless solution.

SDS-PAGE analyses were performed to assess the purity (Fig. 6C left). Relatively, an average 2 mg of total purified his-AGR3-DsRed was yielded from 250 ml of D1 strain culture. The same group of samples were loading in the same gel, running together and performing for a western blot analysis on purified hAD recombinant protein, then stained with a mouse anti-AGR2 monoclonal antibody (Fig. 6C). The main band was detected at the expected molecular weight, confirming the nature and purity of the protein samples.

*Recombinant hAD showed enhanced NIH3T3 cell proliferation and migration*

Through the fluorescence microscopy (Figs. 5, 6A), we have shown the similar auto-fluorescence property of DsRed monomer in hAD recombinant protein. To study the functional properties of AGR2 in hAD, wound healing and CCK-8 assays were performed. Recombinant hAD increased the migration of cells significantly near the wound area compared to untreated group (Fig. 7A). Quantitative analysis showed 1.89 and 2.65 fold increased migration at 24h and 2.0 and 2.69 fold enhanced migration at 48h when treated with 500ng/mL and 1μg/mL of hAD respectively (Fig. 7B). The impact of hAD on cell proliferation was studied using a CCK-8 assay. We treated NIH3T3 cells with different concentrations of hAD and

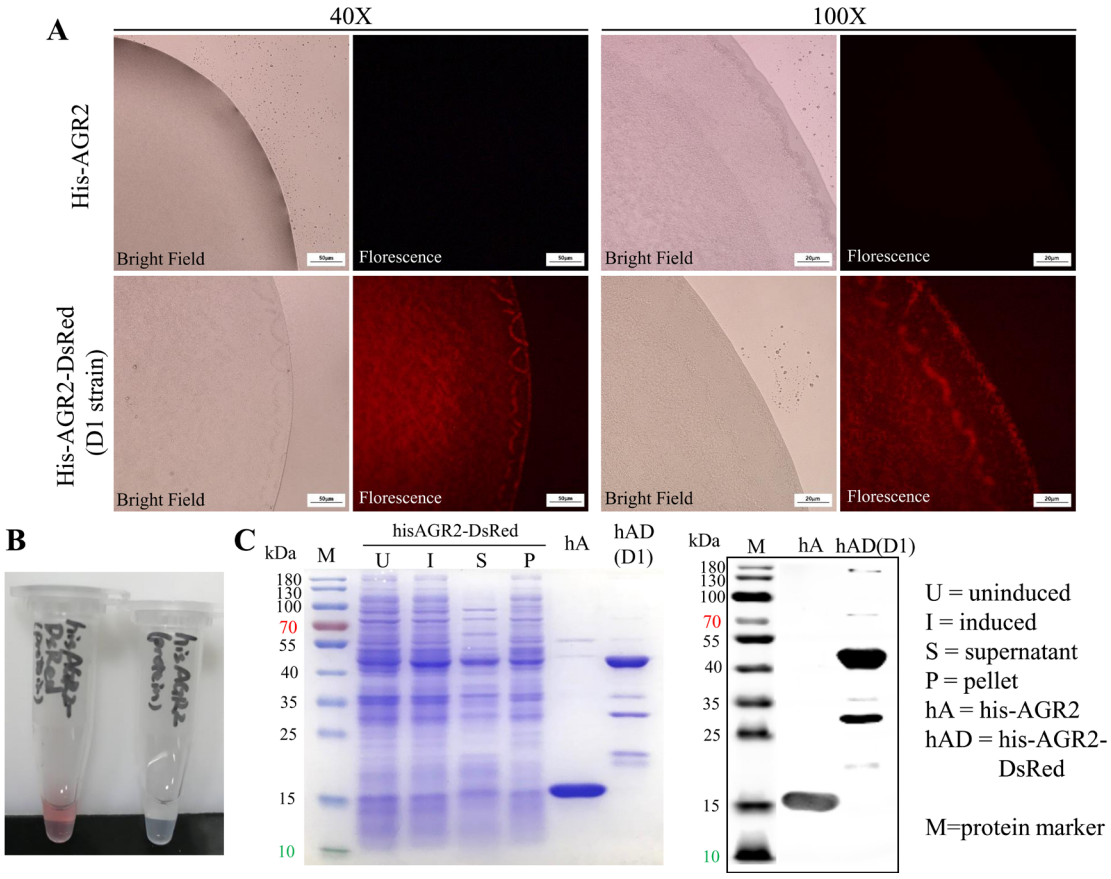


Fig. 6. Recombinant hAD characterized by fluorescence microscopy and Western blot. (A) Bright field and red fluorescence of bacteria culture of his-AGR2 expression strain and hAD expression D1 strain in both 40× and 100× magnifications. Scale bar, 50μm for 40×magnification and 50μm for 100×magnification. (B) Purified his-AGR2 (up) and hAD (down) protein solution, representing different colors. (C) SDS-PAGE and Western blot result of purified hAD, compared with his-AGR2, along with its original expression in bacteria samples. U, uninduced; I, induced; S, supernatant; P, pellet; hA, his-AGR2; hAD, his-AGR2-DsRed; M, protein marker.

detected $OD_{450}$ after 24 hours of incubation, and the result showed that the proliferation rate of cells treated with hAD was increased significantly but no difference between different concentration treatments (Fig. 7C).

*Internalized hAD detected in NIH3T3 and A549 cells*

Extracellular AGR2 plays an important role in tumor microenvironment. We and others have recently reported about the interaction of extracellular AGR2 with various growth factors in tumor microenvironment which affects the intracellular signaling pathways (Guo *et al*., 2017; Jia *et al*., 2018). This could be achieved either by direct or indirect ways.

NIH3T3 cells were treated with hAD in a dose-dependent manner for 24h. Internalization of hAD was detected in the western blot results (Fig. 8A). A549 cells were used to show the intracellular AGR2 expression as a positive control. As hAD's molecular weight is different from native AGR2, this protein can be used for paracrine signaling studies even in the cell lines that express AGR2. We confirmed the fluorescence emission by confocal microscopy which demonstrated the red fluorescence emitted by internalized hAD (Fig. 8B). All these results indicate that hAD is a potential tool to investigate paracrine signaling effect of AGR2 in context of cancer development.

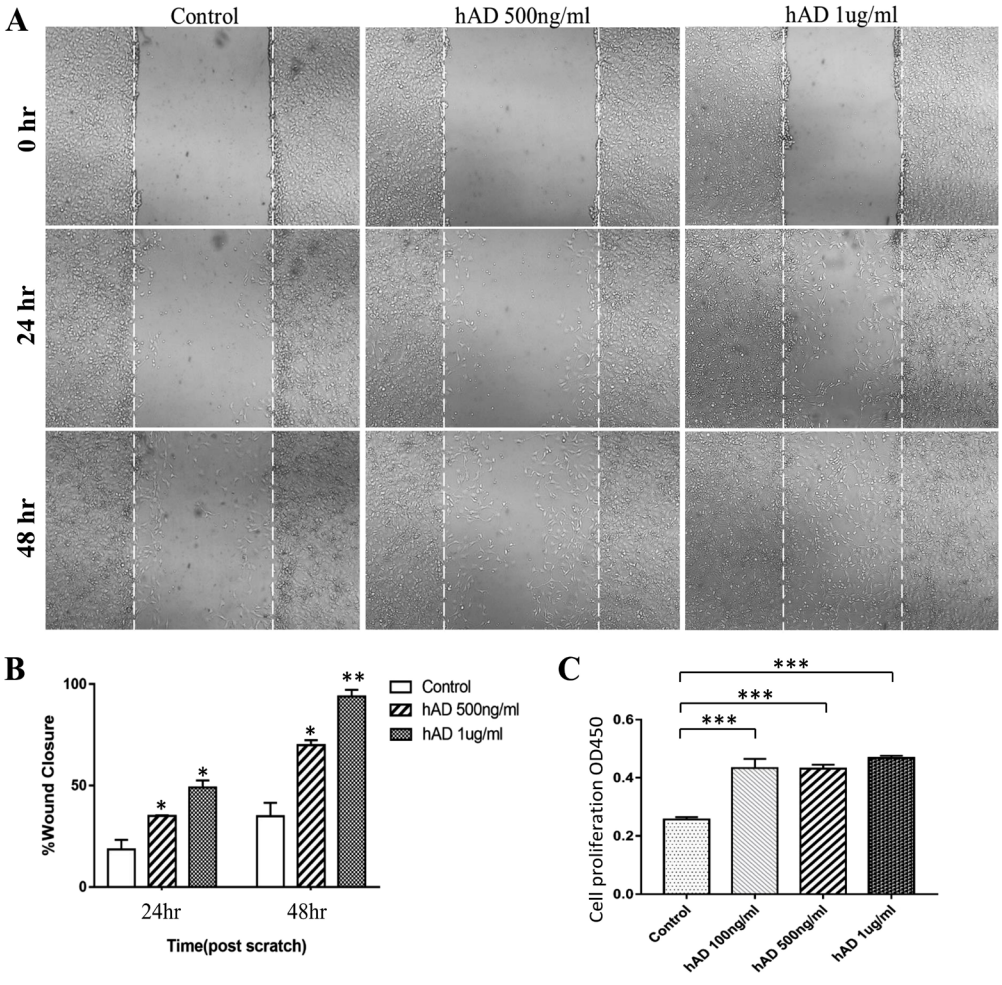


Fig. 7. Recombinant hAD promotes NIH3T3 cell proliferation and migration. (A) Representative images from wound healing assays of NIH3T3 cell cultures treated with hAD demonstrating that cell migration into the cell-free region (outlined) is significantly accelerated in the presence of hAD when compared to controls. Images were captured at 24h and 48h after wounding (magnification, ×100). (B) Bar graph illustrating percentage wound closure at indicated time points during the scratch wound assay in the presence of varying concentrations of hAD (*P = 0.040, *P = 0.020, *P = 0.018, **P = 0.008 versus control). (C) NIH3T3 cell proliferation detected using the Cell Counting Kit-8 assay following treatment with hAD (0, 100, 500 and 1000 ng/mL) after 24h (****P<0.0001, versus the control group).

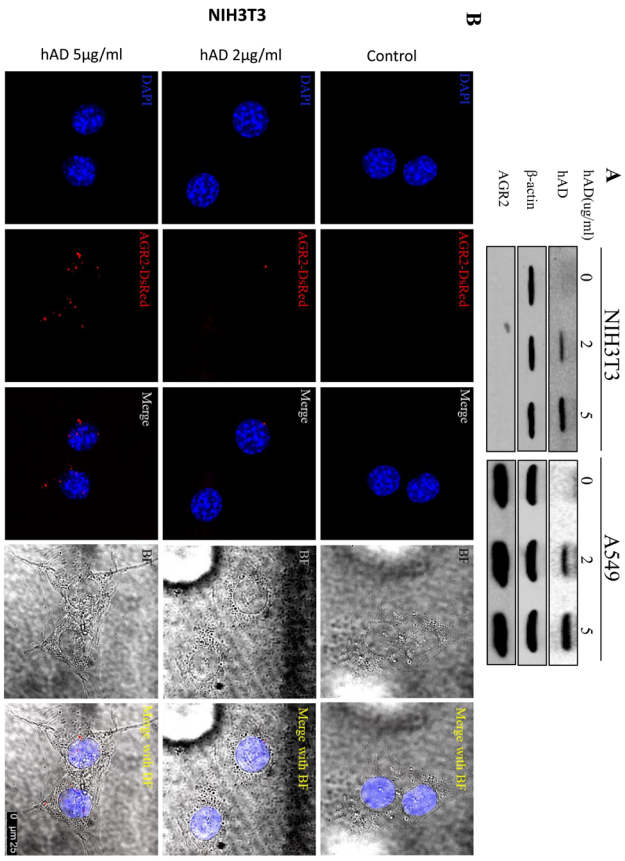


Fig. 8. hAD helps to detect extracellular AGR2 internalization in NIH3T3 cell line which does not have internal AGR2 expression as well as in A549 which express internal AGR2. Cells were treated with different concentrations of hAD for 24h. Internalization of hAD was shown by (A) Western blot analysis. (B) Immunofluorescence assay. Scale bar, 25µm.

## DISCUSSION

Prior work has documented the emerging roles for the pro-oncogenic AGR2 in cancer development, as well as roles involved in asthma, inflammatory bowel disease, cell transformation, cancer drug resistance and metastatic growth (Zheng *et al*., 2006; Li *et al*., 2015, 2016; Fessart *et al*., 2016; Jia *et al*., 2018), and researchers developed a bioactive recombinant AGR2 to investigate the signaling mechanism of this onco-protein. However, various means, especially visualized tools to study the molecular mechanisms and localization of extracellular AGR2 are still main focus in context of the tumor microenvironment. In this study, we designed and obtained a bioactive recombinant AGR2 auto-fluorescent protein successfully.

We performed the construction, expression, purification and characterization of this novel recombinant his-AGR2-DsRed protein using *Escherichia coli* expression system. For the hAD expression and purification, we found that DH5α expression system is more suitable giving better purity than BL21 (DE3) strain. Experimentally both strains showed nearly similar expression of hAD. However, the purification of hAD from both strains using immobilized metal ion affinity chromatography gave different purity profile. We observed the purified protein emitting red fluorescence indicating its potential use for the paracrine signaling studies of AGR2. The hAD's auto-fluorescence might be useful for the live cell imaging and in *in vivo* xenograft model for molecular mechanism studies.

In previous studies, we reported AGR2 enhances proliferation and migration of fibroblasts and keratinocytes (Zhu *et al*., 2017). During the characterization of hAD, the activity check using NIH3T3 cells showed significantly increased proliferation and migration of the fibroblasts indicating hAD as a bioactive recombinant fluorescent protein. In addition, the immunofluorescence emission of the hAD protein observed by immunofluorescent microscopy during prokaryotic expression monitoring indicated the potential applications of hAD for the extracellular AGR2 internalization and cellular localization research. Thus, this study indicates that the properties of recombinant his-AGR2-Dsred auto-fluorescent protein can potentially be utilized to study paracrine signaling mechanism in context of cancer development which will lead to more effective cancer therapies.

However, some limitations are worth noting. DsRed monomer was fused to a location in the C-terminus of human AGR2 in this constructed plasmid, which has been reported to contain ER retention motif, although a linker was inserted, there is a possibility of undesirably functional disturbance. Thus, comparison of DsRed monomer fused at N-terminus of AGR2 needs further investigation. In addition, for the hAD expression in prokaryotic *E.coli* cells, the signal peptide of human AGR2 was deleted. So, further study of recombinant human AGR2 red fluorescent protein obtained from mammalian expression system needs to be done to examine the advantages in native human protein expression.

Although, the potential application of the hAD for the internalization study was shown by immunoblotting and immunofluorescent assays, it needs further experiments to investigate the molecular mechanisms for this phenomenon. Thus, the hAD was expressed successfully in both DH5α and BL21 (DE3) strains, and purified auto-fluorescent hAD bioactive protein showing its novel applications to explore the molecular signaling studies of AGR2.

## CONCLUSION

We have constructed the recombinant hAD fluorescent protein and investigated specific parameters affecting its production to ensure its optimal expression and purification. Using these parameters, hAD was expressed and purified, and the harvested pure protein of high concentrations were checked for the bioactivity and auto-fluorescent. Thus, hAD demonstrates a promising AGR2-DsRed fluorescent recombinant onco-protein that can be applied for the further cancer research.

## ACKNOWLEDGEMENTS

The authors are grateful to Wei Zhang and Sehar Qudsia, University of Shanghai Jiao Tong University, China, for the initial construction of hAD plasmid. This work was supported by the National Natural Science Foundation of China [grant number 81872790]; and Shanghai International Science and Technology Cooperation Program [grant number 184907411400].

*Statement of conflict of interest*

We declare no conflicts of interest in this study.

## REFERENCES

Baird, G.S., Zacharias, D.A. and Tsien, R.Y., 2000. Biochemistry, mutagenesis, and oligomerization of DsRed, a red fluorescent protein from coral. *Proc. natl. Acad. Sci*., **97**: 11984-11989. http://doi.org/10.1073/pnas.97.22.11984

Bevis, B.J. and Glick, B.S., 2002. Rapidly maturing variants of the Discosoma red fluorescent protein (DsRed). *Nature Biotechnol.,* **20**: 83–87. http://doi.org/10.1038/nbt0102-83

Brychtova, V., Vojtesek, B. and Hrstka, R., 2011. Anterior gradient 2: A novel player in tumor cell biology. *Cancer Lett*., **304**: 1-7. http://doi.org/10.1016/j.canlet.2010.12.023

Brychtova, V., Mohtar, A., Vojtesek, B., Hupp, T. R., 2015. Mechanisms of anterior gradient-2 regulation and function in cancer. *Sem. Cancer Biol*., **33**: 16-24. http://doi.org/10.1016/j.semcancer.2015.04.005

Chevet, E., Fessart, D., Delom, F., Mulot, A., Vojtesek, B., Hrstka, R., Murray, E., Gray, T. and Hupp, T., 2013. Emerging roles for the pro-oncogenic anterior gradient-2 in cancer development. *Oncogene*, **32**: 2499–2509. http://doi.org/10.1038/onc.2012.346

Dumartin, L., Whiteman, H. J., Weeks, M. E., Hariharan, D., Dmitrovic, B., Iacobuzio-Donahue, C. A., Brentnall, T. A., Bronner, M. P., Feakins, R. M., Timms, J. F., Brennan, C., Lemoine, N. R. and Crnogorac-Jurcevic, T., 2011. AGR2 is a novel surface antigen that promotes the dissemination of pancreatic cancer cells through regulation of cathepsins B and D. *Cancer Res*., **71**: 7091- 7102. http://doi.org/10.1158/0008-5472.CAN-11-1367

Fessart, D., Domblides, C., Avril, T., Eriksson, L. A., Begueret, H., Pineau, R., Malrieux, C., Dugot-Senant, N., Lucchesi, C., Chevet, E. and Delom, F., 2016. Secretion of protein disulphide isomerase AGR2 confers tumorigenic properties. *eLife*, **5**: e13887. http://doi.org/10.7554/elife.13887

Fritzsche, F.R., Dahl, E., Pahl, S., Burkhardt, M., Luo, J., Mayordomo, E., Gansukh, T., Dankof, A., Knuechel, R., Denkert, G., Winzer, K. J., Dietel, M. and Kristiansen, G., 2006. Prognostic relevance of AGR2 expression in breast cancer. *Clin. Cancer Res.,* **12**:1728-1734. http://doi.org/10.1158/1078-0432.CCR-05-2057

Guo, H., Zhu, Q., Yu, X., Merugu, S.B., Mangukiya, H.B., Smith, N., Li, Z., Zhang, B., Negi, H., Rong, R., Cheng, K., Wu, Z. and Li, D., 2017. Tumor-secreted anterior gradient-2 binds to VEGF and FGF2 and enhances their activities by promoting their homodimerization. *Oncogene*, **36**: 5098–5109. http://doi.org/10.1038/onc.2017.132

Higa, A., Mulot, A., Delom, F., Bouchecareilh, M., Nguyên, D.T., Boismenu, D., Wise, M.J. and Chevet, E., 2011. Role of pro-oncogenic protein disulfide isomerase (PDI) family member anterior gradient 2 (AGR2) in the control of endoplasmic reticulum homeostasis. *J. biol. Chem.,* **286**: 44855-44868. http://doi.org/10.1074/jbc.M111.275529

Ivanova, A.S., Tereshina, M.B., Ermakova, G.V., Belousov, V.V. and Zaraisky, A.G., 2013. Agr genes, missing in amniotes, are involved in the body appendages regeneration in frog tadpoles. *Scient. Rep.,* **3**: 1279. http://doi.org/10.1038/srep01279

Jia, M., Guo, Y., Zhu, D., Zhang, N., Li, L., Jiang, J., Dong, Y., Xu, Q., Zhang, X., Wang, M., Yu, H., Wang, F., Tian, K., Zhang, J., Young, C. Y. F., Lou, H. and Yuan, H., 2018. Pro-metastatic activity of AGR2 interrupts angiogenesis target bevacizumab efficiency via direct interaction with VEGFA and activation of NF-κB pathway. *Biochim. biophys. Acta Mol. Basis Dis*., **1864**: 1622-1633. http://doi.org/10.1016/j.bbadis.2018.01.021

Kuang, W.W., Thompson, D.A., Hoch, R.V. and Weigel, R.J., 1998. Differential screening and suppression subtractive hybridization identified genes differentially expressed in an estrogen receptor-positive breast carcinoma cell line. *Nucl.*

*Acids Res*., **26**: 1116–1123. http://doi.org/10.1093/nar/26.4.1116

Kumar, A., Godwin, J. W., Gates, P. B., Garza-Garcia, A. A. and Brockes, J. P., 2007. Molecular basis for the nerve dependence of limb regeneration in an adult vertebrate. *Science*, **318**: 772-777. http://doi.org/10.1126/science.1147710

Lauf, U., Lopez, P. and Falk, M.M., 2001. Expression of fluorescently tagged connexins: A novel approach to rescue function of oligomeric DsRed-tagged proteins. *FEBS Lett*., **498**: 11-15. http://doi.org/10.1016/S0014-5793 (01)02462-0

Li, Z., Zhu, Q., Hu, L., Chen, H., Wu, Z. and Li, D., 2015. Anterior gradient 2 is a binding stabilizer of hypoxia inducible factor-1α that enhances CoCl 2 -induced doxorubicin resistance in breast cancer cells. *Cancer Sci*., **106**: 1041–1049. http://doi.org/10.1111/cas.12714

Li, Z., Zhu, Q., Chen, H., Hu, L., Negi, H., Zheng, Y., Ahmed, Y., Wu, Z. and Li, D., 2016. Binding of anterior gradient 2 and estrogen receptor-α: Dual critical roles in enhancing fulvestrant resistance and IGF-1-induced tumorigenesis of breast cancer. *Cancer Lett*., **377**: 32-43. http://doi.org/10.1016/j.canlet.2016.04.003.

Lounis, B., Deich, J., Rosell, F.I., Boxer, S.G. and Moerner, W.E., 2002. Photophysics of DsRed, a red fluorescent protein, from the ensemble to the single-molecule level. *J. Physiol. Chem. B*, **105**: 5048-5054. http://doi.org/10.1021/jp010116x

Matz, M.V., Fradkov, A.F., Labas, Y.A., Savitsky, A.P., Zaraisky, A.G., Markelov, M.L. and Lukyanov, S.A., 1999. Fluorescent proteins from nonbioluminescent Anthozoa species. *Nature Biotechnol*., **17**: 969–973. http://doi.org/10.1038/13657

Petek, E., Windpassinger, C., Egger, H., Kroisel, P.M. and Wagner, K., 2003. Localization of the human anterior gradient-2 gene (AGR2) to chromosome band 7p21.3 by radiation hybrid mapping and fluorescencein situ hybridisation. *Cytogenet. Gen. Res*., **89**:141–142. http://doi.org/10.1159/000015594

Pinske, C., Bönn, M., Krüger, S., Lindenstrauß, U. and Sawers, R.G., 2011. Metabolic deficiences revealed in the biotechnologically important model bacterium *Escherichia coli* BL21 (DE3). *PLoS ONE*, **6**: e22830. http://doi.org/10.1371/journal.pone.0022830

Ramachandran, V., Arumugam, T., Wang, H. and Logsdon, C.D., 2008. Anterior gradient 2 is expressed and secreted during the development of pancreatic cancer and promotes cancer cell survival. *Cancer Res*., **68**:7811-7818. http://doi.org/10.1158/0008-5472.CAN-08-1320

Schneider, C.A., Rasband, W.S. and Eliceiri, K.W., 2012. NIH Image to ImageJ: 25 years of image analysis. *Nature Methods*, **9**: 671–675.

Tian, S., Hu, J., Tao, K., Wang, J., Chu, Y., Li, J., Liu, Z., Ding, X., Xu, L., Li, Q., Cai, M., Gao, J., Shuai, X., Wang, G., Wang, L. and Wang, Z., 2018. Secreted AGR2 promotes invasion of colorectal cancer cells via Wnt11-mediated non-canonical Wnt signaling. *Exp. Cell Res*., **364**: 198-207. http://doi.org/10.1016/j.yexcr.2018.02.004

Tsien, R. Y., 1998. The green fluorescent protein. *Annu. Rev. Biochem*., **67**: 509-544. http://doi.org/10.1146/annurev.biochem.67.1.509

Tsuji, T., Satoyoshi, R., Aiba, N., Kubo, T., Yanagihara, K., Maeda, D., Goto, A., Ishikawa, K., Yashiro, M. and Tanaka, M., 2015. Agr2 mediates paracrine effects on stromal fibroblasts that promote invasion by gastric signet-ring carcinoma cells. *Cancer Res*., **75**: 356–66. http://doi.org/10.1158/0008-5472.CAN-14-1693

Zhang, J., Campbell, R.E., Ting, A.Y. and Tsien, R.Y., 2002. Creating new fluorescent probes for cell biology. *Nature Rev. Mol. Cell Biol*., **3**: 906–918. http://doi.org/10.1038/nrm976

Zheng, W., Rosenstiel, P., Huse, K., Sina, C., Valentonyte, R., Mah, N., Zeitlmann, L., Grosse, J., Ruf, N., Nürnberg, P., Costello, C.M., Onnie, C., Mathew, C., Platzer, M., Schreiber, S. and Hampe, J., 2006. Evaluation of AGR2 and AGR3 as candidate genes for inflammatory bowel disease. *Genes Immunity*, **3**: 906–918. http://doi.org/10.1038/sj.gene.6364263

Zhu, Q., Mangukiya, H.B., Mashausi, D.S., Guo, H., Negi, H., Merugu, S.B., Wu, Z. and Li, D., 2017. Anterior gradient 2 is induced in cutaneous wound and promotes wound healing through its adhesion domain. *FEBS J*., **284**: 2856–2869 http://doi.org/10.1111/febs.14155